ONSET OF DISPERSION IN Nb MICROSTRIP TRANSMISSION LINES AT SUBMILLIMETER WAVE FREQUENCIES

H. H. S. Javadi, W. R. McGrath, B. Bumble, H. G. LeDuc

Center for Space Microelectronics Technology
Jet Propulsion Laboratory
California Institute of Technology
Pasadena, CA 91109

ABSTRACT

We have measured the dispersion in phase velocity of a $Nb\text{-}SiO_x\text{-}Nb$ microstrip transmission line resonator over a frequency range from 50 GHz to 800 GHz. A submicron $Nb/Al\text{-}AlO_x/Nb$ Josephson junction was used as a voltage-controlled oscillator to excite the high order modes in the resonator. The same junction is used as a direct detector resulting in a series of step-like structures in the DC current-voltage characteristic at the position of each mode frequency. The transmission line is dispersionless up to about 500 GHz where the phase velocity begins to decrease. This is well below the gap frequency $f_g \approx 700$ GHz. Results agree qualitatively with the expected theoretical behavior near f_g. This onset of dispersion and loss in Nb transmission lines will have a significant impact on the design of submillimeter wave rf circuits.

Superconducting transmission lines have many important applications in high frequency analog circuits and high bit rate digital systems, to name a few. These transmission lines are expected to be nearly lossless and dispersion free up to frequencies near the superconducting energy gap frequency $f_g = 2\Delta / h$, where Δ is the superconductor energy gap parameter and h is Planck's constant. We are interested in superconductive microstrip transmission lines as integrated rf tuning elements for superconductor-insulator-superconductor (SIS) quasiparticle mixers at frequencies near 630 GHz. These SIS mixers provide near quantum-limited sensitivity throughout the millimeter wave band [1-3], provided they are optimized with an appropriate rf embedding circuit. The large geometrical capacitance C_J of the tunnel junction provides a susceptance which shunts the rf signal away from the nonlinear quasiparticle conductance channel. An open-circuited superconductive microstrip transmission line (stub) can provide a parallel inductance to resonate with the junction capacitance. This approach was first used successfully with an SIS mixer operating near 36 GHz [4] and since has been used at frequencies up to 360 GHz [5,6]. However, above 100 GHz, uncertainties in material, transmission line, and junction parameters generally lead to poor performance.

The phase velocity must be accurately known in order to correctly design the microstrip stub for a particular application. At high frequencies possible dispersion and loss are expected to degrade the performance. It is thus important to know the frequency range at which these effects become significant. Other groups [7,8] have measured short-pulse propagation on superconductive coplanar transmission lines using optical sampling techniques and indirectly determined loss and dispersion from a Fourier transform analysis of the pulse distortion.

We have taken a different approach, using a Josephson junction as both a sweep-oscillator and detector to sample the resonances of a microstrip stub. This stub is connected in parallel across the junction as shown in fig. 1. The ac Josephson effect provides a voltage-controlled oscillator. The frequency is $2eV_b/h \approx 0.485 \times V_b$ (μV) GHz where V_b is the junction bias voltage. This monochromatic signal sets up a standing wave in the stub. The junction detects this standing wave and a signature is developed in the DC current-voltage (I-V) curve of the junction by a frequency downconversion process. As the bias voltage, and thus frequency is swept, small current steps will appear in the DC I-V curve of the junction at frequencies corresponding to the modes of the stub. The

frequency spacing of the modes is given by $\Delta f = v_\phi / 2l$ where v_ϕ is the

phase velocity and l is the physical length of the stub. Thus by measuring

the voltage interval between steps, the phase velocity can readily be

obtained if it is constant over this interval. In general, this technique can

be used at high frequencies well above the energy gap frequency f_g. A

similar approach using microstrip resonators with a single resonance

below f_g has recently been reported [9]. Values of surface resistance and

phase velocity were determined up to about 400 GHz. We have used long

microstrip resonators with many high order modes to determine the phase

velocity as a function of frequency up to 800 GHz, which is above the gap

frequency of niobium (Nb). The onset of dispersion has clearly been

observed.

High quality Nb / Al-AlOx / Nb tunnel junctions are fabricated using

a trilayer process [10]. The junction area, defined by electron-beam

lithography, is between $0.3\mu^2$ and $1\mu^2$. The DC sputtered Nb films are 2000 -

3300 Å thick. The current density is as high as 10^4 A/cm^2 and the normal

state resistance is 50Ω - 70Ω. SiO$_x$ serves as both a planarization layer

for the junction trilayer and the dielectric layer for the microstrip stub.

The thickness is $t_d \approx 1500\text{Å}$ and the dielectric constant is taken to be $\varepsilon_r = 5.5$ [11]. The dielectric thickness is comparable to the magnetic penetration depth. In this case, the phase velocity is $<< c$ and hence is strongly affected by the field penetration into the Nb. This makes v_ϕ a sensitive probe of the superconductive properties of Nb.

Junctions fabricated for use as SIS mixers have stubs 2μ wide by 60μ - 70μ long to provide a fundamental broad band resonance near 630 GHz. However, to study the phase velocity, junctions were fabricated with stubs 2μ wide by 518μ or 1064μ long. A longer stub gives a smaller spacing between resonant modes, thus providing a better indication of the phase velocity in a given frequency range. Careful examination of these stubs however, indicated jagged edges and undercutting of the SiO_x. Additional junctions were fabricated with stubs 6μ and 12μ wide to reduce uncertainties due to these edge effects. These stubs were either 500μ, 750μ, or 1000μ long.

The fundamental resonance frequency of a 1000μ long stub is estimated to be about 50 GHz [4]. This leads to steps in the I-V curve which are ≈ 0.1 mV apart. The inset of fig. 2 shows one example. The

subgap conductance of this junction is very large with an almost point-contact type of appearance. While junctions with much lower subgap conductance also showed resonant peaks, the step structure was seen mostly in junctions similar to that shown in fig. 2. An external magnetic field was used to enhance the steps in different voltage ranges [12]. In order to accurately locate these small steps in current, a small amplitude, low frequency (~ 200 Hz) ac voltage was superimposed on V_b. The resulting ac signal was detected with a lock-in amplifier. The interval between two adjacent peaks is then measured to determine v_ϕ which is plotted as a function of the frequency of the higher step. Due to the discreteness of the data, the resolution for changes in velocity is the frequency spacing of the modes. Figure 2 shows the results for 4 different microstrip stubs. About 10 to 14 resonances were observed between 50 GHz and ~ 750 GHz. A smooth curve was drawn through the resulting velocity vs frequency data. The scatter in velocity values about this curve is typically 5%, with only a few points deviating by ~ 10%.

Curve 1 is an example of a junction with a 2μ wide stub. Resonances of these narrow stubs were usually not observable above about 500 GHz. This may be due to increased scattering or losses from the edge effects

mentioned earlier. Curves 2, 3, and 4 represent stubs 1000μ long with widths of 6μ or 12μ. At low frequencies, a slight curvature can been seen in the data as expected from the mode spacing (see discussion below). Otherwise the curves are horizontal up to about 500 GHz where they begin to bend down indicating the onset of dispersion. The gap frequency of a pristine Nb film is $f_g \approx 740$ GHz at 0K. Thus the dispersion begins at frequencies well below f_g. This agrees with previously reported results [8] using an optical sampling technique. While SIS mixers are predicted to operate well up to f_g [13], the resonant embedding circuit utilizing superconductive microstrip transmission lines is limited to lower frequencies.

Figure 3 shows the data for a 500μ long x 12μ wide stub. In this case, resonances, and hence the phase velocity, were obtained up to ≈ 800GHz which is above the gap frequency of Nb. At low frequencies, the velocity is dispersionless. Around 500 GHz, the velocity begins to decrease and reaches its lowest value near 730 GHz. For this data point, the frequency resolution for velocity change is about 50 GHz. This minimum is expected theoretically to occur near 770 GHz (see fig. 3) using a gap frequency of 660 GHz as determined from the I-V curve of this

junction at zero magnetic field (a more complete discussion of the theory will be given in the future [14]). In addition, we have observed a small suppression of the energy gap with external magnetic field in these junctions which may describe the lower frequency of the observed phase velocity minimum. Other loss mechanisms may also play a role. The velocity begins to increase above 730 GHz as is expected theoretically, since the superconductor begins to behave as a normal metal for frequencies well above f_g. The solid line in fig. 3 is the theoretical prediction for the velocity. We have used the approach followed by Kautz [15] which employs the Mattis-Bardeen [16] theory for the electrical conductivity. The magnetic penetration depth was adjusted to $\lambda = 900$Å to fit the theory to the low frequency asymptote of the velocity. As seen from fig. 3, theory and experiment show the same general trend. However, based on the Mattis-Bardeen conductivity, the theory predicts a 9% decrease in velocity at the dip whereas the experiment shows a 35% dip. Errors in velocity resulting from uncertainties in the mode spacings can result from end effects on the microstrip line and the possibility of a negative resistance loop in the I-V curve at the position of the resonance [17]. However for our geometry, the end-effect correction to the length is << 1%, and the worst-case negative resistance, predicted for a lightly-

damped resonance, could only cause a 5% shift in the apparant position of the resonance. Thus neither effect can account for the large change we observe. At low frequencies, superconductive microstrip is a slow-wave transmission line due to the penetration of the electromagnetic field into the superconductor over a length comparable to the thickness of the dielectric. For frequencies well above f_g, the phase velocity increases towards the value for a normal line. The onset of dispersion just below the gap frequency is due to the departure of the imaginary part of the pair conductivity from a 1/f frequency dependence [15].

Some additional insight may be gained by first considering a Josephson junction directly coupled to a lossless microstrip stub. Using the notation in reference [18], the resonant frequencies of the stub are solutions to the transcendental equation

$$-\pi \frac{C_J}{C_S} \frac{f}{f_S} = \tan\left(\frac{\pi f}{f_S}\right) \qquad (1)$$

where $C_S = \varepsilon_r \varepsilon_0 / w / t_d$ is the total capacitance of the stub and f_S is the fundamental mode of the stub. This mode occurs when the length of the

stub,l, equals one wavelength and is given by $f_s = v_\phi / 2l$.

In fig. 4 both sides of eqn. (1) are plotted vs (f/f_s) for an arbitrary value of C_J/C_s. At low frequencies, intersections between the straight line (left hand side of eqn. 1) and the tangent curves are between (m-1/2)f_s and mf_s where m is an integer. These solutions move progressively toward (m-1/2)f_s for $m \gg 1$. Thus at high frequencies, the solutions of eqn. (1) (i.e.: the modes of the stub) are equidistant. If plotted in the spirit of fig. 2, they represent a horizontal line.

We have extended eqn. (1) to the case of a lossy transmission line, yielding

$$-\pi \frac{C_J}{C_s} \frac{f}{f_s} = \frac{2 \sin \left(\frac{2 \pi f}{f_s} \right)}{(e^{2\alpha l} + e^{-2\alpha l}) + \cos \left(\frac{2 \pi f}{f_s} \right)} \qquad (2)$$

where α is the attenuation constant. In fig. 4, the right hand side of eqn.

(2) is plotted for three arbitrary cases of loss: αl = 0.05, 0.10, and 0.15. As can be seen, the distance between the solutions first decreases and then increases as losses in the microstrip line increase. In light of this, our experimental observations can be interpreted as evidence for increased loss in either the superconductor or the dielectric layer. Losses due to radiation will be negligible given the cross sectional dimensions of the stub, 0.15μ x 12μ, compared to relevent free space wavelengths, $\lambda_0 \sim$ 500μ [19]. It is expected that absorption of water in evaporated SiO_x films could contribute losses at microwave and millimeter wave frequencies. Losses due to absorbed water molecules constitute broad peaks in the frequency domain. The attenuation of a microstrip line is linearly proportional to frequency provided the loss in the dielectric is frequency independent. A linear dependence is much weaker than the sharp increase in attenuation expected near the gap frequency. Moreover, since we observe a strong dispersion near the Nb gap frequency, the superconductors are the most probable source for the losses. The superconducting electrodes of the microstrip line are not perfect, defect free, bulk crystalline materials, but are polycrystalline thin films with fine grains and possibly surface layers and interface defects. These

microstructural features of real films may be responsible, in part, for the large dispersion we observe.

In summary, we have presented evidence for the onset of dispersion and loss at submillimeter wave frequencies in Nb-SiO_x-Nb microstrip transmission lines. This behavior is expected at frequencies approaching the gap frequency, but the range over which Nb microstrip lines are dispersionless was previously not well known. These results will have a direct impact on the application of Nb microstrip lines in millimeter wave and submillimeter wave circuits. For operation near 1 THz, higher temperature superconductors such as NbN or NbCN will have to be investigated.

REFERENCES

1. C.A. Mears, Q. Hu, P.L. Richards, A. H. Worsham, D.E. Prober, and A.V. Raisanen, Appl. Phys. Lett. **57**, 2487 (1990).

2. H.H.S. Javadi, W.R. McGrath, S.R. Cypher, B. Bumble, B.D. Hunt, and H.G. LeDuc, Digest, 15th. Int. Conf. on IR and Millimeter Waves, p.245, Orlando, FL (1990).

3. B.N. Ellison, P.L. Schaffer, W. Schaal, D. Vail, and R.E. Miller, Int. J. IR and mm Waves **10**, 937 (1989).

4. A.V. Raisanen, W.R. McGrath, P.L. Richards, F.L. Lloyd, IEEE Trans. Microwave Theory Techn. **MTT-33**, 1495 (1985).

5. Q. Hu, C.A. Mears, P.L. Richards, and F.L. Lloyd, IEEE Trans. Magn. **25**, 1380 (1989).

6. W.R. McGrath, J.A. Stern, H.H.S. Javadi, S.R. Cypher, B.D. Hunt, H.G. LeDuc, IEEE Trans. Magn. **27**, 2650 (1991).

7. M.C. Nuss and K.W. Goossen, IEEE J. Quantum Electronics **25**, 2596 (1989).

8. C.C. Chi, W.J. Gallagher, I.N. Duling III, D. Grischkowsky, N.J. Halas, M.B. Ketchen, and A.W. Kleinsasser, IEEE Trans. Magn. **MAG-23**, 1666 (1987).

9. B. Bi, K. Wan, W. Zhang, S. Han, J.E. Lukens, IEEE Trans. Appl. Superconductivity **1**, 145 (1991).

0. H.G. LeDuc, B. Bumble, S.R. Cypher, and J.A. Stern, submitted to 3rd. International Symposium on Space Terahertz Technology, University of Michigan, Ann Arbor, March 1992.

1. H.K. Olsson, IEEE Trans. Magn. **25**, 1115 (1989).

2. I.O. Kulik, JETP Lett. **2**, 84, 1965.

3. M.J. Feldman, Int. J. IR and mm Waves **8**, 1287 (1987).

4. H.H.S. Javadi and W.R. McGrath, to be published.

5. R.L. Kautz, J. Appl. Phys. **49**, 308 (1978).

6. D.C. Mattis and J. Bardeen, Phys. Rev. **111**, 412 (1958).

7. D.B. Tuckerman and J.H. Magerlein, Appl. Phys. Lett. **37**, 241 (1980).

8. H.D. Jensen, A. Larsen, J. Mygind, IEEE Trans. Magn. **27**, 3355 (1991).

9. T.C. Edwards, *Foundations for Microstrip Circuit Design* , John Wiley and Sons, New York (1981).

FIGURE CAPTIONS

Figure 1.   (a) Geometry of open-circuited microstrip stub and Josephson junction. (b) Cross sectional view of stub and junction.

Figure 2.   Phase velocity vs. frequency for four different Nb microstrip stubs at 4.2K. The stub dimensions are 1: 2μ x 1064μ; 2: 12μ X 1000μ; 3: 6μ X 1000μ;   4: 6μ X 1000μ.   Inset shows current steps in DC IV curve associated with high order modes in the stub.

Figure 3.   Phase velocity vs. frequency for a Nb stub 12μ wide X 500μ long. The different symbols refer to data taken with different applied external magnetic fields. The solid line is the theoretical prediction. The arrow indicates the gap frequency as determined for the Nb junction (at zero magnetic field) which is used in the calculation.

Figure 4.   Graphical representation of both sides of the transcendental eqns (1) and (2). X-axis is frequency normalized to f_s (fundamental resonance of the stub). Straight line is a plot of the left hand side of eqns (1) and (2) with arbitrary slope. Right hand side of eqn (1) is represented by tangent

curves while right hand side of eqn (2) is plotted for values of $\alpha l = 0.05$, 0.10, 0.15. Intersections of the straight line and the tangent curves represent the modes of the stub. When losses are significant ($\alpha l > 0$), the mode frequencies are determined by the closest approach of the two curves as indicated by the arrows.
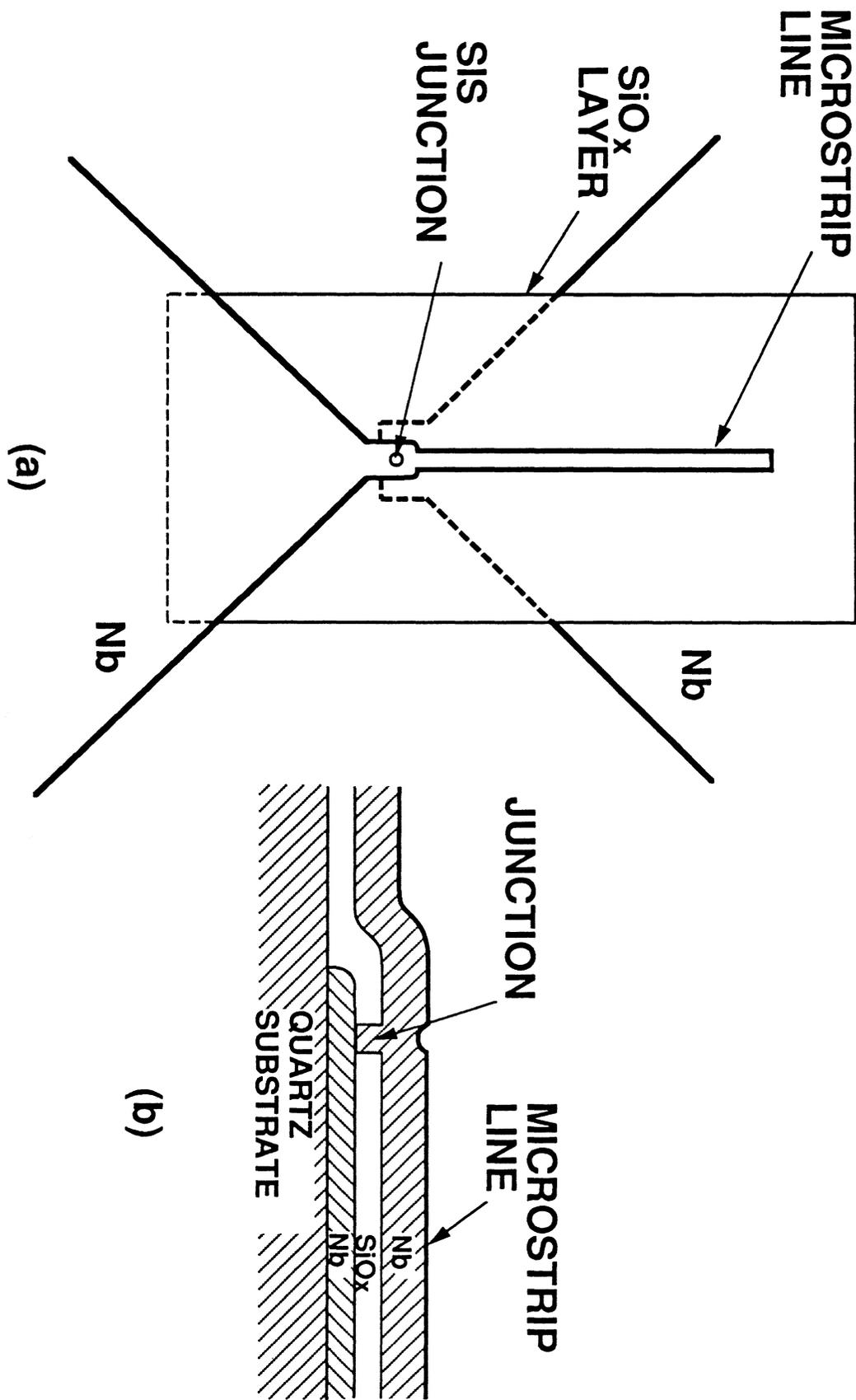
MICROSTRIP
LINE

SiOₓ
LAYER

SIS
JUNCTION

(a)

Nb

Nb

Figure 1

JUNCTION

(b)

QUARTZ
SUBSTRATE

Nb
SiOₓ
Nb

MICROSTRIP
LINE

3

1

−1

−3

−5

−7

−9

−11

−13

−15

slope
$-\pi C_J / C_s$

$\alpha 1 = 0$

$\tan(\pi f / f_s)$

1

n

n+1

n+2

n+3

n+4

f / f$_s$

slope
$-\pi C_J / C_s$

$\alpha 1 = 0$ $\alpha 1 = 0$

$\alpha 1 = 0$

$\alpha 1 = 0.05$

$\alpha 1 = 0.10$

$\alpha 1 = 0.15$